Electron Acceleration and Plasma Instabilities in the Transition Region

F. L. SCARF, W. BERNSTEIN, AND R. W. FREDRICKS

Space Technology Laboratories, Redondo Beach, California

Abstract. It is proposed that after a solar wind enhancement the wind-magnetosphere interface becomes unstable with respect to production of ion acoustic waves. The high frequency electric oscillations then allow plasma to diffuse across the magnetic field, and the waves interact with the electron population via the cyclotron resonance. A small fraction of the electrons are accelerated to kev energies, and the energy distribution function is also distorted in the thermal region. Ultimately, the solar wind becomes locally subsonic with respect to the ion acoustic wave speed, and the waves travel upstream spreading the region of electron thermalization. Various stages in this relaxation process are described, and the theoretical predictions are compared with available experimental results.

1. *Introduction.* In this paper we wish to describe a model of the solar wind–magnetosphere interface in which ion acoustic wave instabilities play an important role. It is argued that the instability produces relaxation of the sheath and that the interface is thus best described as a series of decaying transients. Some properties of ion acoustic waves are briefly summarized in section 2, and their role in producing temporal variations is discussed in section 3. An ion acoustic wave–gyrofrequency resonance which can generate superthermal electrons is described in the next section, and the experimental situation is reviewed in section 5.

It is concluded that these instabilities and the associated temporal variations are important in the solar wind–magnetosphere interface and that the concept of a fixed and well-defined transition region is not a useful one. For instance, in the presence of ion acoustic waves thermal and superthermal electron 'boundaries' should differ from each other and from ion and/or magnetic field 'boundaries.' We also anticipate that field boundaries generally depend strongly on the sampling rate, the kind of averages taken, etc., and it is argued that instruments with different windows and sensitivities will generally observe boundary phenomena at different ranges. Many of the available experimental results appear to support these conjectures.

2. *Properties of ion acoustic waves.* The steady-state interaction between the solar wind and an interplanetary obstacle such as the magnetosphere is governed by collective effects, even if the size of the obstacle is small compared with the mean free path in the streaming plasma. This is so because waves generated in the interface can travel upstream and distort the incident flow from the Newtonian or independent particle pattern which is associated with the Chapman-Ferraro (C-F) sheath. In trying to account for the collective effects, we must consider all modes of wave propagation in the transition region, examine the probable significance of each mode (i.e., the spectral intensity), and compare the wave velocity with the local wind speed for each kind of wave.

The waves usually considered to be most important in this respect are the Alfvén and magnetoacoustic oscillations; however, in a warm plasma, the purely longitudinal or 'electrostatic' mode with

$$\mathbf{E} = -\nabla\phi \qquad \phi = \phi_0 \cos(\mathbf{k}\cdot\mathbf{r} - \omega t) \qquad (1)$$

appears most readily.

In the presence of a uniform magnetic field $\mathbf{B} = B\mathbf{i}_z$, the full dispersion relation for a collisionless plasma is extremely complex [*Stix*, 1962, chapters 8, 9], but some of the main features of these waves can be stated simply if we consider only propagation parallel to the magnetic field, $\mathbf{k} = k\mathbf{i}_z$. For $T_e \gg T_i$ and $k \lesssim k_D^{(i)} = (4\pi N e^2/\kappa T_i)^{1/2}$, the zero damped dispersion relation for interpenetrating Maxwellians (electrons drifting through ions with relative speed V) has the approximate form

$$\frac{1}{\omega^2} \simeq \frac{m_i}{k^2 \kappa T_e} + \frac{1}{\Omega_p^2} \qquad (2)$$

where Ω_p is the ion plasma frequency [*Stix*, 1962, p. 214]. For $\omega \ll \Omega_p$ these waves grow spontaneously if V exceeds the phase velocity, $(\omega/k) \simeq (\kappa T_e/m_i)^{1/2}$, and for $\omega \simeq \Omega_p$ equation 2 is approximately satisfied with $k \simeq k_D^{(i)}$ $(T_e/T_i \gg 1)$, but the critical drift speed is reduced to $\Omega_p/k_D^{(i)} \simeq (\kappa T_i/m_i)^{1/2}$. The complete threshold curve for $V_c = V_c(T_e, T_i)$ is given in Figure 2 of *Bernstein, Fredricks, and Scarf* [1964] (henceforth referred to as BFS) and this can be used to show, for instance, that if $T_e/T_i \gtrsim$ (10–15) with $T_i \simeq 2 \times 10^5$ °K, then any electron-ion drift speed greater than (100–150) km/sec will be sufficient to trigger the ion acoustic wave instability. In fact, it is known [*Stix*, 1962, p. 223] that these theoretical calculations greatly overestimate the stability of a real collisionless plasma with respect to ion acoustic wave generation, and that low frequency signals (i.e., ion waves with $\omega < \Omega_p$) are observed even when a small current is passed through a collisionless plasma with $T_e = T_i$.

In BFS the role of the ion wave instability in producing relaxation of a C-F sheath was considered qualitatively. It was assumed that the electron plasma instability discussed by *Piddington* [1960] produces local electron thermalization, $\kappa T_e \rightarrow \frac{1}{2}(m_i u_0^2/2) \gg \kappa T_i$, so that a C-F sheath becomes unstable with respect to ion acoustic wave generation, allowing fast diffusion of charged particles across the geomagnetic field [*Spitzer*, 1960]. On this basis, predictions concerning the ultimate 'steady-state' configuration were presented in BFS. In the present note, we wish to extend the picture in several ways: (1) We recognize that the transition region magnetic field can produce local charge separation electric fields over the entire transition region, so that electron heating via the two-stream instability can occur upstream from the magnetopause. In fact, if low frequency magnetic disturbances (Alfvén and magnetoacoustic waves) propagate upstream to produce magnetic disorder with locally nonvanishing $(\mathbf{E} + \mathbf{u} \times \mathbf{B})$, then the development outlined in BFS should yield $T_e/T_i \gg 1$ throughout the region. (2) We observe that the instability and associated sheath relaxation imply that the interface is intrinsically time dependent, and it is argued that the sheath is best described as a series of decaying transients initiated by changes in the solar wind. (3) We consider the role of ion acoustic waves in reducing the local Mach number. If κT_e attains its maximum local value, $m_i u_0^2/4$, then the ion acoustic wave phase velocity, $(\kappa T_e/m_i)^{1/2}$, is comparable to the incident solar wind speed. Distortions in the electron distribution function, perturbations in the solar wind speed or composition, etc., can then produce locally sonic conditions so that magnetosonic and ion acoustic waves propagate upstream, spreading the region of high electron temperatures. (4) It is observed that in the transition region the ion acoustic wave spectrum $(0 < \omega < \Omega_p^i)$ extends up into the kilocycle range, overlapping the local electron gyrofrequency. Under these conditions, the longitudinal electric oscillations can accelerate some electrons to superthermal energies by a modified cyclotron mechanism.

3. *Temporal variations.* The Mariner plasma probe [*Snyder et al.*, 1963] and magnetometer [*Coleman et al.*, 1962] data show that interplanetary conditions are rarely constant for periods longer than several hours, even during nonstorm days, and this is confirmed by the Explorer 18 observations [*Ness et al.*, 1964]. Moreover, the gross changes in wind velocity do not appear to be correlated with immediate surface geomagnetic activity; instead the geomagnetic 'noise' level appears to be simply related to the magnitude of the wind velocity. These facts can support a theory that the interface is always unstable and that the gross fluctuations merely change the nature and state of the instability by delivering varying amounts of energy to the interface and by initiating a new decaying transient; as the sheath relaxes, the local currents produce low frequency magnetic disturbances.

With these comments in mind, it is useful to describe the wind-magnetosphere interaction as a series of transients and to contemplate the development of the interface after a sudden enhancement in solar wind flux has compressed the magnetosphere and swept away any flux of quasi-trapped particles. At $t = 0$, the subsolar field and flux profiles should resemble those predicted by the C-F theory (Figure 1*a*). Collisions are unimportant, and, very soon after the enhancement occurs, waves produced near the interface cannot significantly distort the

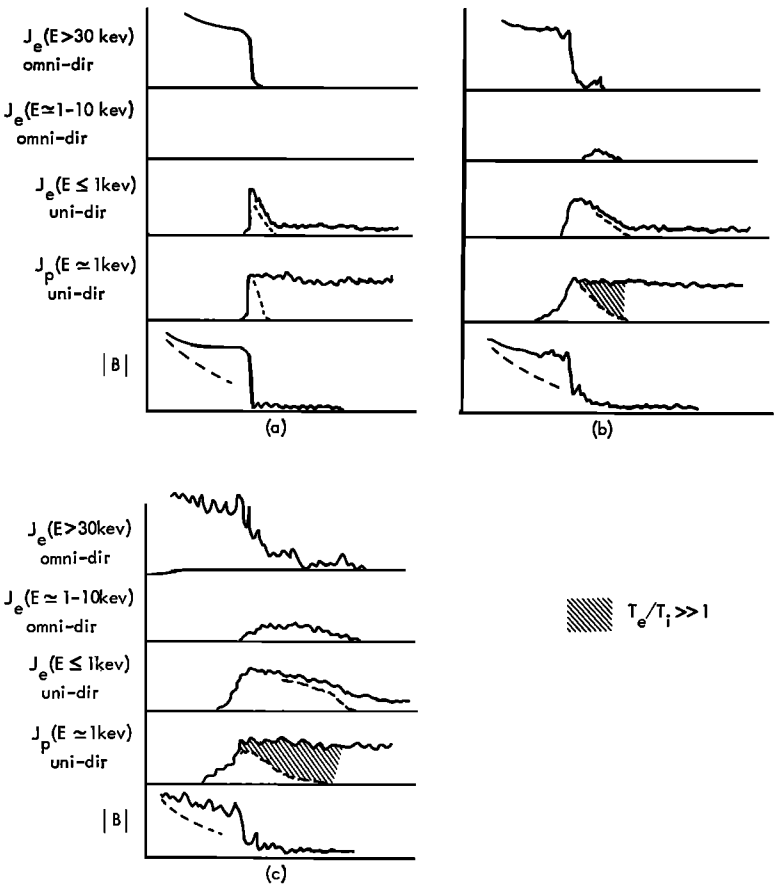

Fig. 1. The predicted formation and decay of the solar wind–magnetosphere interface after a wind enhancement has produced a transient Chapman-Ferraro sheath. The shaded region has $T_e/T_i \gg 1$. The solid unidirectional curve represents solar-directed flux, the dotted curve is antisolar, and the time development proceeds from (*a*) to (*c*). The disorder in $|B|$ is supposed to represent high frequency, small amplitude perturbations associated with electrostatic ion waves. Large amplitude low frequency fluctuations (not shown) are related to the development indicated here through the relation $\nabla \times \mathbf{B} = \mathbf{j}$.

Newtonian flow by interacting with particles which have not yet arrived.

At later times low frequency Alfvén waves generated in the sheath of Figure 1*a* can begin to travel upstream, scatter and heat the incoming particles, and ultimately produce a momentary quasi-shock front; the term 'quasi-shock' describes the case in which the electrons are heated and thermalized throughout a specific transition region while the ion thermalization is primarily completed near the inner boundary. It takes some time for this interface to develop, and the growth time must certainly exceed $t_1 = |r_2 - r_1|/V_A$, the time needed to propagate an Alfvén wave from a magnetopause (r_1) to a shock front (r_2) (for $|r_2 - r_1| \simeq 4R_e$, $V_A \simeq 70$ km/sec, $t_1 \approx 6$ minutes). The true growth time should be considerably longer than t_1, however, because the electrons are to be completely thermalized, and appropriate currents must be set up. Since the magnetic field is also disordered beyond the magnetopause (see section 5), it is likely that the effective Alfvén speed is considerably smaller than $\sqrt{(B^2/4\pi Nm)}$, where B is the average field in the transition region.

We anticipate that the configuration shown in Figure 1*b* develops in a time of the order of hours after a sudden enhancement and that at this stage the electrons are thermalized and heated as soon as they penetrate into a specific

transition region but that the ions merely lose drift energy near the outer boundary. Nearer to r_1 ion heating must occur, and here both κT_e and κT_i tend toward $\frac{1}{4}m_i u_0^2$. In the outer crosshatched region, however, $T_e/T_i \gg 1$, and thus almost any small current can trigger the ion wave instability. If a significant steady transverse magnetic field component is locally present, charge separation electric fields are strong enough to induce the threshold current (see BFS) and stimulate the waves. The magnetic field fluctuations indicated in Figure 16 are thus high frequency small amplitude ($\Delta B \simeq \omega \Delta E/kc^2$) oscillations associated with ion acoustic waves. Of course, large amplitude low frequency fluctuations (not shown) are also present. If the electrons are thermalized first, this low frequency noise will be associated ($\nabla \times \mathbf{B} = \mathbf{j}$) with deflection and thermalization of the ion stream as it approaches the magnetospheric obstacle.

In Figure 1c a hypothetical later stage in the relaxation is schematically depicted. On the upstream side of the crosshatched region in Figure 1b it was assumed that the ions remain cool but lose of the order of half their streaming energy ($u \rightarrow u_0/\sqrt{2}$), which goes into thermalization of the electrons $\kappa T_e \rightarrow m_i u_0^2/4$. If this does happen, the local 'ion wave Mach number,' $u/(\kappa T_e/m_i)^{1/2}$, is reduced to $\sqrt{2}$ and the local magnetosonic Mach number is even lower, since this phase velocity is increased to [*Stix*, 1962, p. 200]

$$V_{M.S.} \simeq \left\{ \frac{B^2}{4\pi N m_i} + \left[\frac{2\kappa T_i}{m_i} + \frac{\kappa T_e}{m_i} \right] \sin^2 \theta \right\}^{1/2} \tag{3}$$

Here $|\mathbf{k} \times \mathbf{B}| = kB \sin \theta$, and it has been assumed that both distribution functions are isotropic and Maxwellian. Under these circumstances the local flow is nearly sonic, and small changes in solar wind composition or speed can allow the waves to begin propagating upstream. If the collisionless electron thermalization leads to an isotropic distribution with a significant non-Maxwellian tail, the Mach number is further reduced, since the ion acoustic wave speed then becomes

$$\frac{\omega}{k} \rightarrow \left(\frac{\gamma_e \kappa T_e}{m_i} \right)^{1/2} \tag{4}$$

where γ_e is a shape-dependent parameter greater than unity, and anisotropies can also distort the Mach numbers. Thus, it seems reasonable to contemplate that waves propagating upstream short distances will thermalize incoming electrons, producing further upstream disturbances, etc., so that the outer boundary of the transition region will slowly spread upstream, relaxing as indicated in Figure 1c.

Ion acoustic waves can also enter the magnetosphere freely in regions where they need not propagate across the magnetic field at wide angles. This suggests that the magnetopause may be relatively well defined near the subsolar point but that ion waves may be found in the outer magnetosphere away from the noon meridian and equator. In these outer regions we would expect to find high frequency ($0 < f < f_p$ (ion) $\simeq$ 1 kc/s) longitudinal electric oscillations, solar plasma diffusing into the magnetosphere, and thermal (whistler) plasma diffusing outward into the transition region.

These 'electrostatic' waves may be expected to produce small numbers of superthermal electrons when certain resonance conditions are met (see section 4), and this effect is also schematically represented in Figure 1 by the drawings of $E > 30$ kev electron fluxes.

The temporal variability of the wind-magnetosphere interface is an essential point of our argument, so that many different configurations are predicted; however, these cases have some fundamental features in common. In particular, it is expected that, with the exclusion of a short time period following a wind enhancement, a region with $T_e/T_i \gg 1$ exists because the massive protons cannot respond to perturbations as rapidly as the electrons. If this region also contains a finite magnetic field perpendicular to the ion streaming speed and steady for a time long compared to ion wave periods ($\approx 10^{-3}$ sec), then currents produced by the charge separation electric fields are large anough to generate the ion wave instability and associated electric field fluctuations induce superthermal heating of some electrons.

4. *Electron acceleration mechanisms.* In this section we wish to consider in more detail the possible superthermal acceleration of a small fraction of the electron population by the ion acoustic waves. The phenomena discussed here were suggested by a description of an electron cyclotron–electron plasma wave interaction recently considered by *Stix* [1964] in an attempt

to account for the production of 100-kev electrons in laboratory beam-plasma experiments [*Smullin and Getty*, 1962; *Alexoff et al.*, 1963].

The longitudinal waves can be described by a potential function (equation 1) with $\omega = \sqrt{\delta_e \kappa T_e/m_i}\, k$ and $0 < k < k_D$[i]. In the presence of an external magnetic field $\mathbf{B}_0$, the equation of motion for an electron is

$$m_e \frac{d\mathbf{v}}{dt} = e\mathbf{k}\phi_0 \sin(\mathbf{k}\cdot\mathbf{r} - \omega t) - e\mathbf{v}\times\mathbf{B}_0/c \tag{5}$$

For simplicity, let us first examine an idealized case with $\mathbf{B}_0 = B_0\mathbf{i}_z$, $\mathbf{k} = k\mathbf{i}_x$. Equation 5 yields

$$\ddot{y} = \dot{x}\omega_c \tag{6}$$

$$\ddot{x} = (ek\phi_0/m_e)\sin(kx - \omega t) - \dot{y}\omega_c \tag{7}$$

with $\omega_c = eB_0/m_e c$. Equation 6 gives $\dot{y} - x\omega_c =$ constant, and for those electrons for which the constant vanishes,

$$\ddot{x} + \omega_c^2 x = \frac{ek\phi_0}{m_e}[\sin kx\cos\omega t - \cos kx\sin\omega t] \tag{8}$$

For small excursions ($kx \ll \pi/2$) equation 8 becomes

$$\ddot{x} + \omega_c^2 x - \frac{ek^2\phi_0}{m_e} x\cos\omega t \simeq \frac{-ek\phi_0}{m_e}\sin\omega t \tag{9}$$

and the right-hand side can be regarded as the driving term; in this case, it is of interest to examine the solutions to the homogeneous equation

$$\ddot{x} + \left[\omega_c^2 - \frac{ek^2\phi_0}{m_e}\cos\omega t\right]x = 0 \tag{10}$$

Equation 10 is the Mathieu equation, and it is known that for certain ranges of the parameters unstable growing solutions are found. We define $2\tau = \omega t$ and rewrite (10) in the standard form

$$(d^2x/d\tau^2) + (b - h^2\cos^2\tau)x = 0$$

with $b = 4\omega_c^2/\omega^2$, $h^2/2 = 4ek^2\phi_0/m_e\omega^2$; the unstable regions in the b-h plane are given, for instance, by *Morse and Feshbach* [1953]. For $h \ll 1$ (very small ion wave electric fields), the unstable regions are quite narrow and they are centered around $b = n^2$, $n = 1, 2, \cdots$, so that growth occurs if $\omega = 2\omega_c/n$; since the inhomogeneous driving term also oscillates with frequency ω, we can expect extremely rapid acceleration when the resonance conditions are met.

This linearized treatment is, of course, a gross oversimplification of the nonlinear problem. However, it does illustrate the initial growth of the electron motion. In addition to the linear approximation, the low frequency disorder in $\mathbf{B}_0$ has been ignored. Moreover, in very strong magnetic fields $\mathbf{k}\times\mathbf{B}_0 \simeq 0$ since ion waves are guided along field lines; in weak fields first-order corrections to the $\mathbf{B}_0 = 0$ dispersion relation are small and hence $\mathbf{k}\times\mathbf{B}_0$ need not be small. More realistic calculations have now been carried out on an analog computer, and a detailed discussion of these results will appear [*Fredricks et al.*, 1965]; equation 5 has been solved for cases with $\mathbf{k}\cdot\mathbf{B}_0 \neq 0$, and a long coherence time for $\mathbf{B}_0$ was introduced. The numerical analysis indicates that moderate ion wave fields which have $\frac{1}{2}\omega$ near a suitable Doppler shifted ω_c are quite effective in producing kev particles in short times even when $\mathbf{k}\cdot\mathbf{B}_0 \neq 0$, although small $k_\parallel/k_\perp$ still produces the greatest acceleration. When $k_\parallel \neq 0$, the mean particle drift velocity along the field must be related to the speed with which the ion wave propagates along $\mathbf{B}_0$, and this requirement limits the energy transfer. Near the subsolar point $k_\parallel$ is indeed small for inward propagation, but the ion waves are highly attenuated in a fairly narrow 'magnetopause' so that small fluxes of high energy electrons should be produced steadily. Away from this region $k_\parallel/k_\perp$ is not so small, and we might therefore expect production of softer electrons over long times.

It is again assumed here that the large amplitude $\mathbf{B}_0$ fluctuations of (section 5) have coherence times long compared with ion wave periods (milliseconds) so that reasonably small electric fields have enough time to produce high energy electrons. If the $|\Delta\mathbf{B}/\mathbf{B}_0| \simeq 1$ fluctuation periods are also of the order of milliseconds, then little superthermal acceleration would be expected, but the $\mathbf{B}$ fluctuations with kilocycle frequencies produced by the ion waves should generally have very small amplitudes.

5. *Comparison with experiment.* The most complete measurements of the outer magnetosphere and the transition region were made using the sensitive, high resolution detectors on

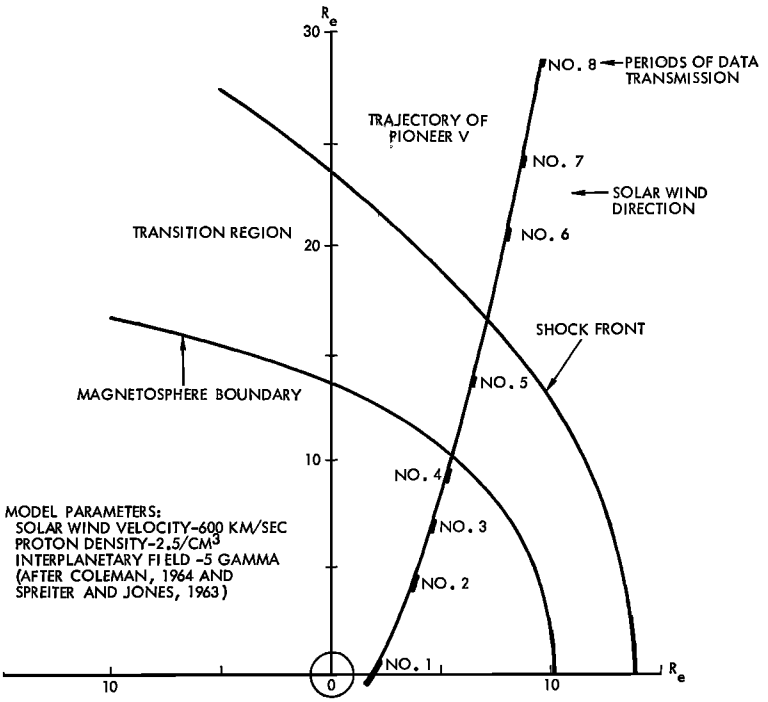

Fig. 2. Approximate trace of a theoretical magnetosphere boundary and a shock front in the plane of the trajectory of Pioneer 5. The boundaries were calculated by *Sprieter and Jones* [1963] for a solar wind of 2.5 photons/cm^3 and 600 km/sec with a magnetic field of 5 γ. The spacecraft transmitted data from positions indicated by the heavy dashes [*Coleman*, 1964].

Explorer 18, but only scattered and preliminary discussions of the results are presently available. However, important characteristics of this region were determined on earlier flights, and it is now possible to make some comparison between theory and experiment for the sunlit hemisphere.

The earliest magnetometer indications of an extremely broad, disordered and complex transition region are derived from the Pioneer 1 [*Sonett et al.*, 1960] and Pioneer 5 [*Coleman*, 1964] data. In Figure 2 the trajectory and the locations of the first eight periods of Pioneer 5 data transmission are shown and are compared with reasonable theoretical magnetopause and shock front boundaries derived from the work of *Spreiter and Jones* [1963]. The experimental values for $B_\perp$ are shown in Figure 3 for six transmissions of interest, and the instantaneous values are compared with the extrapolated dipolar values. It is possible to make a fairly unambiguous identification of the $8.5R_e$ results with a geomagnetic field which is slightly compressed, and at $30R_e$ the moderately quiet field has a value which agrees with the interplanetary value of Mariner 2 [*Coleman et al.*, 1962]. However, the entire region between at least 10.5 and $25.4R_e$ appears to be a highly disordered transition region. In particular, transmission 4, which is supposed to occur within the hypothetical magnetopause, exhibits rapid large field fluctuations, and very similar effects are seen through transmissions 6 and 7, which are supposed to be beyond the shock front. There is no real evidence for a discontinuity in $B_\perp$ between transmissions 5 and 6 (the average field, however, is somewhat closer to geomagnetic for 6), and there is no evidence for quiet conditions upstream of a shock at about $18R_e$. Of course, these one-component measurements refer to a single pass during a moderately disturbed period, and no properties of the wind were measured; however, the Pioneer 5 data rate of 1 point per 1.5 sec was considerably higher than those of subsequent high precision magnetometers, and therefore

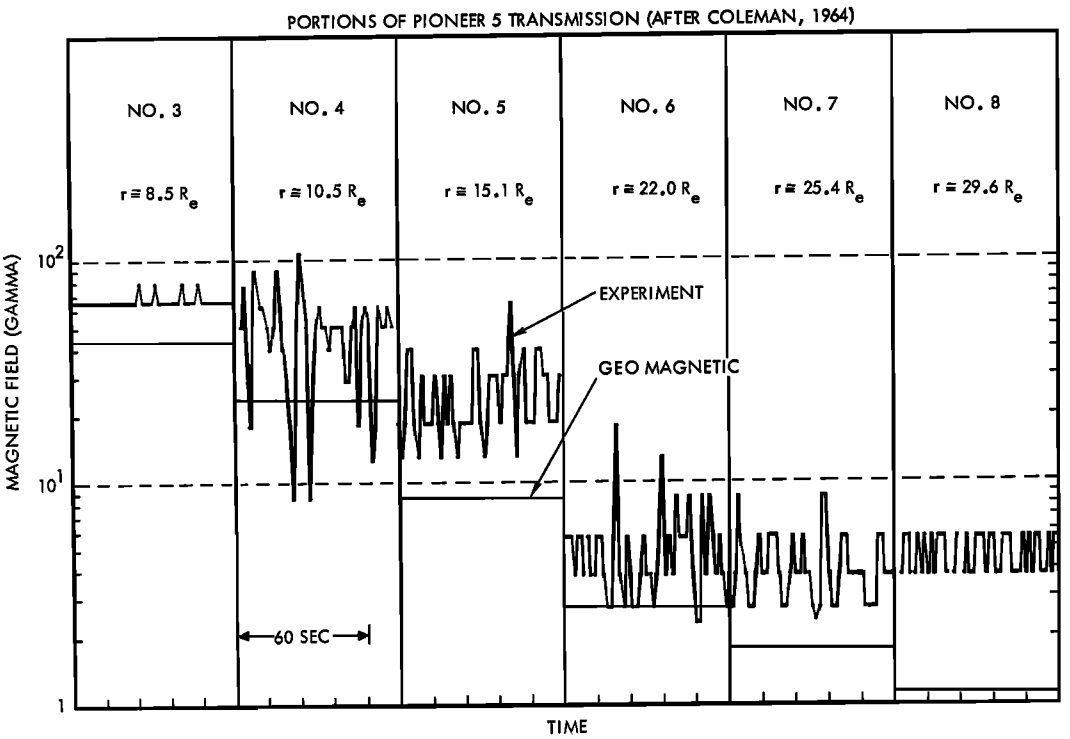

Fig. 3. Measurements of the magnetic field recorded from Pioneer 5 during transmissions 3–8 [after *Coleman*, 1964]. The points shown represent sequences of individual measurements obtained during parts of the indicated transmission periods. The measurements were obtained at 1.5-sec intervals, and the solid curve represents the value of the appropriate component expected from the geomagnetic field.

these relatively high frequency fluctuations may uniquely indicate the true size of the transition region.

The next probe to investigate the sunlit hemisphere was Explorer 12, and the CdSTE detector on the satellite measured [*Freeman et al.*, 1963; *Freeman*, 1964] an extremely broad and variable region ($r_1 \simeq$ 5.2 to 6.4 $\times$ 10^4 km, $r_2 \simeq$ 6.5 to $>$8.4 $\times$ 10^4 km, $0 < L_{sep} < 70°$) populated by large particle fluxes ($J \simeq 10^8$–10^{10}/cm² sec); it was argued that these were electrons with $E \simeq$ 0.5 to 2–3 kev. The inner boundary of this thermalization region appeared to be associated with termination of magnetospheric electron flux (40 kev $< E <$ Mev) and with the onset of large amplitude magnetic fluctuations. However, $r_1 = r_1(\theta, \phi, u_0, t)$ was not always well defined (particularly away from $L_{sep} = 0°$), and r_2 was generally (i.e., on 25 out of 38 inbound passes) beyond the apogee of Explorer 12 (83,600 km).

In this belt, the electrons undoubtedly acquire the maximum thermal energy allowed by equipartition ($\kappa T_e \simeq \frac{1}{4} m_p u_0^2$), so that we must discuss an enormously broadened ($\delta \simeq$ 10,000 km to $>$25,000 km) wind-magnetosphere interface. However, not enough information is available from the Explorer 12 detectors to confirm or deny the predictions of Figure 1. There was nearly always some indication of simultaneous changes in the total energy flux and the magnetic field parameters (J. Freeman, private communication), but the large uncertainties in the magnetic field measurements [*Cahill and Amazeen*, 1963] preclude a detailed correlation study. Furthermore, the plasma probe which might have yielded T_e/T_i gave apparently inconsistent results, and the 40 to 50-kev detector was not sufficiently sensitive to measure the presence of a superthermal high energy tail in the transition region.

Nevertheless, other evidence does suggest that more sensitive instruments would rarely (if ever) measure a sharp boundary for thermalized

electrons or other transition region phenomena. The retarding potential analyzer on Explorer 18 [*Serbu*, 1964] found $J(E > 100 \text{ ev}) \simeq 10^7 \text{ cm}^2$ sec at $7R_e$ and $J(E > 100 \text{ ev}) \geq 2 \times 10^8/\text{cm}^2$ sec for $8R_e < r < 16R_e$ during an outbound pass (Nov. 27, 1963) for which the magnetometer indicated a magnetopause near $11.3R_e$. The inner boundary discrepancy of 18,000 to 25,000 km suggests significant inward diffusion of hot electrons from a source beyond $11\text{–}12R_e$, and fast diffusion across a magnetic field is consistent with the presence of an ion wave instability (BFS). (Night-side measurements may reveal similar broadening; Explorer 12 and Lunik 2 [*Gringauz et al.*, 1961] detected a belt of thermalized electrons past $7\text{–}9R_e$, while whistler analysis [*Liemohn and Scarf*, 1964] indicates a small but significant flux of 200 ev $< E <$ 3 kev electrons between 2.5 and $4.5R_e$.)

The region mapped by Explorer 14 excluded the neighborhood of the subsolar point, and a detector capable of observing electrons with $E < 40$ kev was not used. Nevertheless, the high energy electron detectors yielded important information about the structure, extent, and temporal variation of the outer magnetosphere and the transition region. The main results [*Frank et al.*, 1963, 1964] which have bearing on a discussion of the sunlit hemisphere might be summarized as follows:

1. Large fluxes of low energy (40 kev $< E <$ 200 kev) superthermal electrons are present throughout the magnetosphere. The typical flux at $L = 4.0$, $\theta_m \simeq 0$ is about $3 \times 10^7 \text{ cm}^{-2} \text{ sec}^{-1}$, but variations by a factor of 100 are seen in periods of the order of days. The fluctuation amplitude increases markedly with increasing L and is positively correlated with K_p peaks. The soft electron flux increases within a day after the onset of a storm, and it recedes to its pre-storm value within about a week. There is definite evidence of rapid diffusion of enhanced electron fluxes across magnetic shells, but the proton population is considerably more stable.

2. The boundary of the magnetosphere as indicated by the SUI 213A GM detector is relatively well defined for the early inbound passes of Explorer 14 [*Frank et al.*, 1963, Figures 1 and 2], although discrete and variable local enhancements of $E > 40$ kev electrons appear near the boundary. Farther away from the subsolar region (for instance on the outbound passes with $\theta_m \simeq 15\text{–}30°$, $L_{sep} > 70°$) a termination of the $E > 40$ kev flux is not found out to apogee (98,000 km), but beyond about 50,000 km short-term spatial and temporal flux variations of an order of magnitude are customarily encountered.

3. Occasionally large isolated superthermal (40 kev $< E <$ 200 kev) electron flux enhancements appear far beyond the normal boundary. For instance, on Oct. 6–7, 1962, the SUI 213A counter detected an electron flux of $2 \times 10^5 \text{ cm}^{-2} \text{ sec}^{-1}$ at a range of $90\text{–}95 \times 10^3$ km, or 20,000 km past the apparent magnetosphere boundary. Of course the Explorer 14 instruments would not detect such bursts if (*a*) $E < 40$ kev; (*b*) $J(E > 40 \text{ kev}) \lesssim 2 \times 10^4 \text{ cm}^{-2} \text{ sec}^{-1}$ (see Figure 4); (*c*) $r > 98{,}500$ km. Thus, only limited information can be obtained from this satellite. Moreover, the very large flux observed at short range on Oct. 6–7 should not necessarily be regarded as typical.

The preliminary Explorer 18 results further illuminate the transition region phenomena in several significant ways. For electron energies above about 50 kev, the University of Chicago charged particle detector (CPD) should be more sensitive than a counter such as SUI 213A. The CPD window corresponds to an energy loss of ~30 kev, and the discriminator requires ~130 kev to detect an event. Therefore electrons of energy 30–160 kev can only be detected as a result of 'pile-up,' as discussed by *Fan et al.* [1964], and this is confirmed by the laboratory calibration; a flux of $J = 2.5 \times 10^5 \text{ cm}^{-2} \text{ sec}^{-1}$ ($N = 2.5 \times 10^6 \text{ sec}^{-1}$) 47-kev electrons yields 10 c/s. An idealized and simplified generalization of this 'pile-up' calibration can be constructed if we use Poisson statistics and assume a constant resolving time T. The count rate in the presence of a monoenergetic beam is then

$$C_R = [N(NT)^m/m!] \exp(-NT) \qquad (11)$$

where N is the incident flux, and $m(E) \geq 130/[E \text{ (kev)} - 30]$ is the number of electrons needed to give a count. The 47-kev calibration yields $T \simeq 3.5 \times 10^{-7}$ sec, and the computed curve for $C_R[J(E), E] = 10$ is shown in Figure 4 together with the idealized SUI 213A threshold. For a variety of reasons, the true sensitivity of the CPD is probably considerably better than the function shown in Figure 4. In particular, if local wave motions produce particle bunching,

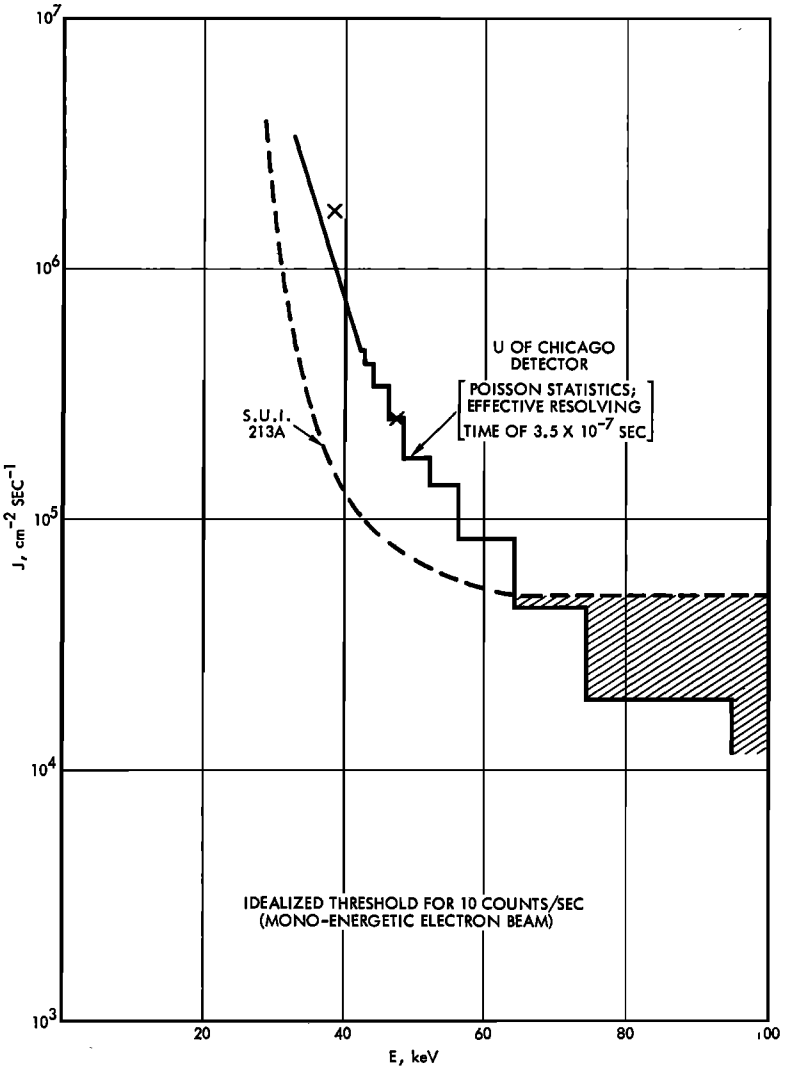

Fig. 4. Comparison of idealized threshold curves, $C_R[J(E), E] = 10$ c/s, for the SUI 213A GM counter and the University of Chicago charged particle detector. The crosses represent laboratory calibration points [*Fan et al.*, 1964], and the University of Chicago detector has a lower flux threshold in the shaded regions. The idealized 213A calibration is based on discussions by *Frank* [1962] and *Frank et al.* [1963].

then much lower values of $J(E)$ will be detected.

Even on the basis of equation 11, however, the CPD flux threshold is lower than that of the Geiger counter above about 60 kev, and because of its nonlinear response [e.g., $C_R \sim N^3 \exp(-NT)$] the CPD can give a clear spike above background where a less sensitive linear detector would measure a fairly small ripple, or no increase over background.

For these reasons, the CPD observations of localized peaks of high energy electrons at great distances from the magnetosphere boundary are particularly significant. Let us consider the data from the first twelve inbound passes of Explorer 18 as being most representative of conditions near the subsolar point. On each of these inbound passes a sudden increase in the 5.46-minute Cartesian variance of the magnetic field was detected and identified as 'the collisionless shock wave' by *Ness et al.* [1964], although

occasionally increases in the variance were detected upstream. On four of these twelve passes (4, 6, 8, and 11) the CPD detected no spikes, and the plasma probe indicated an indefinite boundary for thermalization of the solar wind ions (J. H. Wolfe, private communication). On passes 5, 7, and 9 the CPD spikes were detected near the main magnetic variance decrease, and the probe indicated that ion thermalization occurred at approximately the same range. However, on the remaining five passes, distant CPD electron spikes were detected from 6000 km to 40,000 km *upstream* from the magnetic variance decrease; in these cases the ion thermalization boundary was sometimes indefinite but it was generally located near the magnetic 'boundary.' The CPD peaks are usually less than 5000 km thick, the flux levels are correlated with the degree of disturbance of the geomagnetic field, and the location is highly variable both spatially and temporally.

We interpret the increase in the 5.46 magnetic variance as an indication that the ions (which contribute the main local currents if the electrons have already been thermalized) are being deflected and gradually thermalized as the stream approaches the magnetospheric obstacle. We interpret the distant CPD spikes as superthermal electrons produced by ion acoustic waves (kilocycles) which may have traveled upstream from the main electron thermalization region. The energy is dissipated as the wave enters a region of quiet magnetic fields and a large spike is produced when the local value of $(\mathbf{k}\cdot\mathbf{B})$ becomes small. The CPD calibration suggests that the spikes are probably real. If E were 30–40 kev, then C_R would go as N^{m+1} exp $(-NT)$ with $m > 12$, so that a very small ripple above threshold ($J > 5 \times 10^5$ cm^{-2} sec^{-1}) would appear as a huge spike. However, this would imply an energy flux of 2×10^{10} ev/cm^2 sec, although an incident solar wind with $N_p = 5$ cm^{-3}, $E_p = 2$ kev only delivers 6.2×10^{11} ev/cm^2 sec. It is more reasonable to believe that at these large ranges the particle energies are of the order of 60–80 kev, so that $J \simeq 5 \times 10^4$ cm^{-2} sec^{-1} (or less if bunching occurs) and the energy flux is then certainly less than 1% of the solar wind flux. Near the magnetosphere boundary where some sort of trapping occurs, it is more likely that large fluxes of lower energy ($E \simeq 30$ kev) particles can exist, and in this region some of the CPD spikes may indeed be highly magnified ripples.

More definitive interpretations of these electron measurements must await detailed calibration studies and comparison with the response of the University of California Geiger counter on Explorer 18 [*Anderson et al.*, 1964]. The latter is a type 213 GM tube with a gold foil backscattering arrangement which provides a 5-kev electron energy loss so that the response should be roughly similar to that shown in Figure 4 with a 5-kev shift toward higher energies. The CPD and the GM tube generally detected different boundaries for magnetosphere trapping, and this can be reasonably explained by considering variations in effective threshold energy (30 kev versus 45 kev) and also the very nonlinear CPD response at the lower energies.

However, the origin of apparent discrepancies in the readings beyond the 5.46-min magnetic variance decrease is much more obscure. On the first six *inbound* passes, the GM tube detected an upstream 'spike' only once (pass 2). The peak flux was 7×10^3/cm^2 sec, it lasted for 17 minutes, it was located about $2R_e$ upstream of the magnetic 'boundary' [*Ness et al.*, 1964], and it was also detected by the CPD [*Fan et al.*, 1964]. However, on passes 1 (in) and 3 (in), the CPD found upstream spikes which were apparently not recorded by the GM tube. These differences suggest again that the energies of distant superthermal electrons are in the crossover region of Figure 4 ($E \simeq$ 50–70 kev), but it would also appear that the true sensitivities of the detectors may differ considerably from the idealized curves for a monoenergetic flux of independent isotropic electrons.

Finally, it is worth noting that the largest upstream electron flux detected by the GM tube occurred near apogee ($r \simeq 31.6R_e$) in connection with a severe local magnetic disturbance. On pass 2 (out), a sudden magnetic fluctuation with fields as high as 15 γ was encountered at a distance $15R_e$ upstream from the magnetic 'shock wave.' Somewhat later the GM tube detected an electron flux of 10^4/cm^2 sec which lasted for two minutes.

In many respects, these results tend to support the theory outlined in sections 2, 3, and 4. The variability of the $E > 40$ kev magnetospheric electron flux and its positive correlation with ΣK_p (or u_0) suggest that these superthermal

particles are generated somewhere in the transition region. The fluctuations observed near the 'magnetosphere boundary' can then represent the main source regions where ion waves dissipate and accelerate the thermalized electrons, but the observed rapid diffusion across the geomagnetic field is consistent with the presence of a finite ion wave amplitude throughout the outer magnetosphere. (The subsequent conversion of $E > 40$ kev electrons to $E > 1.6$ Mev fluxes could then be associated with an iteration of the acceleration process within the magnetosphere, although the original Stix mechanism [electron plasma oscillation—electron cyclotron interaction] may be more relevant here than the ion acoustic wave resonance.) The large localized flux enhancements detected far beyond the magnetopause suggest that ion waves generated in the transition region do travel upstream and locally accelerate the electrons when the magnetic field becomes transverse and quiet.

6. *Conclusions.* None of the results quoted above directly confirms the basic assumption of our theory that ion acoustic waves exist in the transition region. However, certain suggestive conclusions about the sunlit interface can be drawn from the data at hand:

1. The transition region and magnetosphere characteristics are highly variable and sensitive to variations in solar wind flux.

2. Superthermal particles are produced in the transition region and outer magnetosphere. The acceleration process frequently occurs far upstream from the region of ion thermalization and related low frequency large amplitude magnetic disturbance.

3. The designation of the location of the 'magnetopause' or the 'shock front' appears to depend greatly on the type of detector as well as on the range and sensitivity of the instrument.

We feel that all these facts are consistent with the instability-acceleration mechanism described in BFS and in the present paper. In fact, if the physical processes which operate in the interface involve the complex phenomena discussed here (ion wave instabilities, unequal temperatures, fast diffusion, nonlinear wave-particle interactions, non-Maxwellian distributions, superthermal accelerations) there is no reason to expect various measurements to be at all correlated in space or in time. For instance, low frequency magnetic fluctuation analysis ($T \geq$ minutes) should not reveal the boundaries of the ion wave region ($T \simeq 10^{-3}$ sec), and so any limits established by such a study will generally be unrelated to those suggested by examination of high energy electron fluxes. By the same token, the extent of the ion thermalization region should not generally indicate where wind electrons are thermalized, or be related to the limit of magnetospheric trapping, and the separate limit of the whistler plasma. Furthermore, if ion waves of sizeable amplitudes ($\phi_0 > 100$ volts) are present in the transition region, the interpretation of low energy (say $E = 0$–2 kev) ion and electron measurements becomes somewhat obscure.

Acknowledgments. We are indebted to J. W. Freeman, J. H. Wolfe, and E. N. Parker for helpful discussions, and to K. Anderson, P. J. Coleman, Jr., N. F. Ness, G. P. Serbu, J. A. Simpson, and T. H. Stix for making their reports available to us in advance of publication.

One of the authors (Bernstein) has been supported in part by the Air Force Office of Scientific Research under contract AF 49(638)-886; the other authors have been supported by the National Aeronautics and Space Administration under contract NASw-698.

References

Alexeff, I., R. V. Neidigh, W. F. Peed, E. D. Shipley, and E. G. Harris, Hot electron plasma by beam-plasma interaction, *Phys. Rev. Letters, 10*, 273, 1963.

Anderson, K. A., H. K. Harris, and R. J. Paoli, Energetic electron fluxes in and beyond the earth's outer magnetosphere, *Rept. Ser. 5, Issue 50, Phys. Dept. and Space Sci. Lab., Univ. Calif.*, Berkeley, September 1964.

Bernstein, W., R. W. Fredricks, and F. L. Scarf, A model for a broad disordered transition between the solar wind and the magnetosphere, *J. Geophys. Res., 69*, 1201, 1964.

Cahill, L. J., and P. G. Amazeen, The boundary of the geomagnetic field, *J. Geophys. Res., 68*, 1835–1843, 1963.

Coleman, P. J., Jr., Characteristics of the region of interaction between the interplanetary plasma and the geomagnetic field: Pioneer 5, *J. Geophys. Res., 69*, 3051–3076, 1964.

Coleman, P. J., Jr., L. Davis, Jr., E. J. Smith, and C. P. Sonett, Mariner 2: Interplanetary magnetic fields, *Science, 138*, 1099, 1962.

Fan, C. Y., G. Gloeckler, and J. A. Simpson, Evidence for >30 kev electrons accelerated in the shock transition region beyond the earth's magnetospheric boundary, *Phys. Rev. Letters, 13*, 149–153, 1964.

Frank, L. A., Efficiency of a Geiger-Müller tube for non-penetrating electrons, *J. Franklin Inst., 273,* 91–106, 1962.

Frank, L. A., J. A. Van Allen, and H. K. Hills, A study of charged particles in the earth's outer radiation zone with Explorer 14, *J. Geophys. Res., 69,* 2171–2191, 1964.

Frank, L. A., J. A. Van Allen, and E. Macagno, Charged particle observations in the earth's outer magnetosphere, *J. Geophys. Res., 68,* 3543, 1963.

Fredricks, R. W., F. L. Scarf, and W. Bernstein, Numerical estimates of superthermal electron production by ion acoustic waves in the transition region, *J. Geophys. Res., 70*(1), January 1, 1965.

Freeman, J. W., The morphology of the electron distribution in the outer radiation zone and near the magnetospheric boundary as observed on Explorer 12, *J. Geophys. Res., 69,* 1691, 1964.

Freeman, J. W., J. A. Van Allen, and L. J. Cahill, Jr., Explorer 12 observations of the magnetospheric boundary and associated solar plasma on September 13, 1961, *J. Geophys. Res., 68,* 2121, 1963.

Gringauz, I. I., V. V. Bezrukikh, V. D. Ozerov, and R. E. Rybchinskii, A study of the interplanetary ionized gas, high energy electrons, and corpuscular radiation from the sun by means of the three-electrode trap for charged particles on the second Soviet cosmic rocket, *Soviet Phys. Dokl., English Transl., 5,* 361, 1961.

Leimohn, H. B., and F. L. Scarf, Whistler determination of electron energy and density distributions in the magnetosphere, *J. Geophys. Res., 69,* 883, 1964.

Morse, P. M., and H. Feshbach, *Methods of Theoretical Physics,* part 1, p. 563, McGraw-Hill Book Company, New York, 1953.

Ness, N. F., C. S. Scearce, and J. B. Seek, Initial results of the Imp 1 magnetic field experiment, *J. Geophys. Res., 69,* 3531–3569, 1964.

Piddington, J. H., Geomagnetic storm theory, *J. Geophys. Res., 65,* 93–105, 1960.

Serbu, G. P., Results from the Imp-1 retarding potential analyzer, *NASA Rept. X-615-64-109, Goddard Space Flight Center,* May 1964.

Smullin, L. D., and W. D. Getty, Generation of a hot, dense plasma by a collective beam-plasma interaction, *Phys. Rev. Letters, 9,* 3–6, 1962.

Snyder, C. W., M. Neugebauer, and U. R. Rao, The solar wind velocity and its correlation with cosmic-ray variations and solar and geomagnetic activity, *J. Geophys. Res., 68,* 6361, 1963.

Sonett, C. P., D. L. Judge, A. R. Sims, and J. M. Kelso, A radial rocket survey of the distant geomagnetic field, *J. Geophys. Res., 65,* 55–68, 1960.

Spitzer, L., Jr., Particle diffusion across a magnetic field, *Phys. Fluids, 3,* 659–660, 1960.

Spreiter, J. R., and W. P. Jones, On the effect of a weak interplanetary magnetic field on the interaction between the solar wind and the geomagnetic field, *J. Geophys. Res., 68,* 3555, 1963.

Stix, T. H., *The Theory of Plasma Waves,* McGraw-Hill Book Company, New York, 1962.

Stix, T. H., Energetic electrons from a beam-plasma overstability, *Matt-239, Plasma Physics Lab., Princeton Univ.,* February 1964.

(Manuscript received July 9, 1964;
revised October 8, 1964.)